

# Constraints on the Universal Varying Yukawa Couplings: from SM-like to Fermiophobic

---

Tianjun Li,<sup>a,b</sup> Xia Wan,<sup>c</sup> You-kai Wang,<sup>a</sup> and Shou-hua Zhu<sup>c,d</sup>

<sup>a</sup>*State Key Laboratory of Theoretical Physics and Kavli Institute for Theoretical Physics China (KITPC), Institute of Theoretical Physics, Chinese Academy of Sciences, Beijing 100190, P. R. China*

<sup>b</sup>*George P. and Cynthia W. Mitchell Institute for Fundamental Physics, Texas A&M University, College Station, TX 77843, USA*

<sup>c</sup>*Institute of Theoretical Physics & State Key Laboratory of Nuclear Physics and Technology, Peking University, Beijing 100871, China*

<sup>d</sup>*Center for High Energy Physics, Peking University, Beijing 100871, China*

*E-mail:* [tli@itp.ac.cn](mailto:tli@itp.ac.cn), [xia.wan@pku.edu.cn](mailto:xia.wan@pku.edu.cn), [wangyk@itp.ac.cn](mailto:wangyk@itp.ac.cn), [shzhu@pku.edu.cn](mailto:shzhu@pku.edu.cn)

ABSTRACT: Varying the Standard Model (SM) fermion Yukawa couplings universally by a generic positive scale factor ( $F_{Y_u}$ ), we study the phenomenological fit to the current available experimental results for the Higgs boson search at hadron colliders. We point out that the Higgs production cross section and its decay branching ratio to  $\gamma\gamma$  can be varied oppositely by  $F_{Y_u}$  to make their product almost invariant. Thus, our scenario and the SM Higgs are indistinguishable in the inclusive  $H \rightarrow \gamma\gamma$  channel. The current measurements on direct Yukawa coupling strength in the  $H \rightarrow b\bar{b}/\tau\tau$  channel are not precise enough to fix the scale factor  $F_{Y_u}$ . The most promising is the vector-boson-fusion channel in which the CMS has already observed possible suppression effect on the Yukawa couplings. Furthermore, the global  $\chi^2$  fit of the experimental data can get the optimal value by introducing a suppression factor  $F_{Y_u} \sim 1/2$  on the SM Yukawa couplings.

---

## Contents

<b>1</b>	<b>Introduction</b>	<b>1</b>
<b>2</b>	<b>The model</b>	<b>3</b>
<b>3</b>	<b>Numerical results</b>	<b>4</b>
<b>4</b>	<b>Conclusion</b>	<b>9</b>
<b>5</b>	<b>Supplement</b>	<b>10</b>

---

## 1 Introduction

Even though the Standard Model (SM) has achieved an impressive phenomenological success, the Higgs mechanism, which breaks the electroweak gauge symmetry and gives masses to the electroweak gauge bosons, has not been confirmed. The Higgs mechanism also gives masses to the SM fermions through the Yukawa couplings, which are equal to the fermion masses times the inverse of the vacuum expectation value (VEV) of the Higgs field. However, the Yukawa couplings do not provide any explanation for the observed large hierarchy in the fermion masses.

Recently, both the CMS and ATLAS Collaborations have released a series of results about the Higgs searches in  $\gamma\gamma$ ,  $WW$ ,  $ZZ$ ,  $b\bar{b}$  and  $\tau\tau$  decay modes [1–4]. The CMS experiment excluded the 127.5–600 GeV at 95% confidence level while observed an excess with a global significance of  $1.6\sigma$  after look-else-where effect for a Higgs boson mass hypothesis of 125 GeV in the  $\gamma\gamma$  mode [3]. The ATLAS experiment gives a consistent result of observing an excess with a significance of  $1.5\sigma$  at 126.5 GeV in the  $\gamma\gamma$  mode [4]. ATLAS also see small excesses in  $ZZ \rightarrow 4l$  channel [4] at 125 GeV while CMS shows some slight excesses in  $ZZ \rightarrow 4l$  channel at 119.5 GeV and 320 GeV [3]. Moreover, Tevatron gives a CDF and D0 combination result of observing an excess of  $2.2\sigma$  in  $WH/ZH$  and  $H \rightarrow b\bar{b}$  channels [5]. Besides confirming or excluding these hints experimentally, the urgent problem is to check whether this 125 GeV possible Higgs boson is SM-like or belong to the other SM extensions.

One kind of new physics scenario is the so-called fermiophobic Higgs model [6–16], in which the Higgs boson does not couple to the SM fermions while its couplings to the gauge bosons are the same as the SM. The SM fermions can acquire masses by other mechanisms rather than the Yukawa couplings. At the LHC, the fermiophobic Higgs production cross section is much lower than the SM, but its branching ratio to diphoton increases, thus the experimental observable cross section  $\sigma(pp \rightarrow H + x) \cdot \text{Br}(H \rightarrow \gamma\gamma)$  is slightly changed. The detailed numbers are shown in table 1. Recently, both CMS and ATLAS have performed searches for the fermiophobic Higgs boson [1, 17, 18]. For CMS, in Ref. [1], by combining

Channels	SM	FP	$Ratio(FP/SM)$
$\sigma(pp \rightarrow H + x)$	17.50pb	2.19pb	12.51%
$Br(H \rightarrow \gamma\gamma)$	0.23%	1.54%	6.70
$Br(H \rightarrow W^+W^-)$	21.63%	86.89%	4.02
$Br(H \rightarrow ZZ)$	2.65%	10.85%	4.10
$Br(H \rightarrow b\bar{b})$	57.54%	0	0
$Br(H \rightarrow \tau\tau)$	6.30%	0	0
$\sigma(pp \rightarrow H + x) \cdot Br(H \rightarrow \gamma\gamma)$	0.04pb	0.034pb	0.84
$\sigma(pp \rightarrow H + x) \cdot Br(H \rightarrow W^+W^-)$	3.79pb	1.90pb	0.50
$\sigma(pp \rightarrow H + x) \cdot Br(H \rightarrow ZZ)$	0.46pb	0.24pb	0.51
$\sigma(pp \rightarrow H + x) \cdot Br(H \rightarrow b\bar{b})$	10.70pb	0	0
$\sigma(pp \rightarrow H + x) \cdot Br(H \rightarrow \tau\tau)$	1.10pb	0	0

**Table 1.** Production cross section and decay branching ratios of SM and fermiophobic Higgs for the mass of 125 GeV at 7 TeV  $pp$  collision .

different decay channels, the fermiophobic Higgs boson is excluded in the mass range 110-192GeV at 95% CL. While, analysis in diphoton decay mode with lepton-tagged or dijet-tagged [17] shows there is a small excess of fermiophobic Higgs with  $1.2\sigma$  global significance around 126 GeV. ATLAS has also observed an excess of fermiophobic Higgs at 125.5 GeV, with a global significance of  $1.6\sigma$  in diphoton decay mode [18].

In the Standard Model, fermions and gauge bosons get their masses from Yukawa couplings and Higgs kinetic term, respectively. The Higgs boson, which was initially introduced to have a nonzero VEV, provides the SM fermion masses via different Yukawa couplings. Theoretically, there are quite a few new physics models that have modified Yukawa couplings. Phenomenologically, we just introduce a generic positive factor  $F_{Y_u}$  on the SM Yukawa couplings for all the SM fermions<sup>1</sup>. The standard model is recovered when  $F_{Y_u} = 1$ , and it is the pure fermiophobic case when  $F_{Y_u} = 0$ . As the coupling strength is modified, the SM fermions should get their mass by other scenarios or Higgs field. The simplest way is to put a  $SU(2)_L \times U(1)_Y$  breaking term  $m_q \bar{q}_L q_R$  [21]. Other possible solution can be realized by, as suggested in Ref. [21], the ‘‘Extended technicolor’’. To be model independent, We will not go though in the details of such models here.

In this paper, we consider the universal varying SM fermion Yukawa couplings by a generic positive scale factor. We discuss the phenomenological fit to the current available hadron collider Higgs boson search experimental results, and find that the optimal fit gives the  $F_{Y_u} \sim 0.5$ . Interestingly, the Higgs production cross section and its decay branching ratio to  $\gamma\gamma$  can be varied oppositely so that their product is almost invariant. Thus, the inclusive  $H \rightarrow \gamma\gamma$  decay channel information is not enough to confirm the SM Higgs boson. The current experimental results on direct Yukawa coupling channels  $H \rightarrow b\bar{b}/\tau\tau$  are not precise enough to determine the scale factor. The most promising channel is the vector boson fusion since the CMS Collaboration has shown that the SM fermion couplings are

<sup>1</sup>Generically, a negative factor can also be valid. Such as discussed in [19, 20]. We will compare positive and negative  $F_{Y_u}$  in the following sections.

probably smaller than the SM.

The paper is organized as follows: in section 2, we describe the models and related formulas for Higgs production and decay channels at the LHC. Section 3 presents the numerical results and comparison with experimental results for the 125 GeV Higgs. Section 4 is the conclusion. Because the ATLAS and CMS collaborations at the LHC announced the discovery of a new Higgs-like boson before the publication of the paper, we add an update supplementary analysis in section 5.

## 2 The model

As we only introduce a modified factor on the Yukawa coupling, the Higgs couplings to the gauge bosons are unchanged. At the LHC, the dominant SM Higgs production process is the gluon-gluon fusion channel, via a heavy quark triangle vertex diagram. This process can be seriously changed by the modified Yukawa factor. The leading order production cross section can be described as [22]:

$$\sigma_{LO}^{gg}(pp \rightarrow H + x) = \sigma_0^H \tau_H \frac{d\mathcal{L}^{gg}}{d\tau_H} \quad \text{with} \quad \frac{d\mathcal{L}^{gg}}{d\tau} = \int_x^1 \frac{dx}{x} g(x, \mu_F^2) g(\tau/x, \mu_F^2), \quad (2.1)$$

where  $\tau_H = M_H^2/s$  with  $s$  being the invariant collider energy squared,  $g(x, \mu_F^2)$  is the parton-distribution-function and  $\mu_F$  is the factorization scale. The parton level cross section  $\sigma_0^H$  is

$$\sigma_0^H = \frac{G_F \alpha_s^2(\mu_R^2)}{288\sqrt{2}\pi} \left| \frac{3}{4} \sum_Q F_{Y_u} A_{1/2}^H(\tau_Q) \right|^2, \quad (2.2)$$

where  $F_{Y_u}$  is the modified Yukawa coupling factor,  $G_F$  is the Fermi constant,  $\alpha_s$  is the strong coupling constant,  $\mu_R$  is the renormalization scale, and  $\tau_Q = M_H^2/4m_Q^2$ . The quark amplitude  $A_{1/2}^H(\tau)$  is

$$A_{1/2}^H(\tau) = 2[\tau + (\tau - 1)f(\tau)]\tau^{-2}. \quad (2.3)$$

The function  $f(\tau)$  is,

$$f(\tau) = \begin{cases} \arcsin^2 \sqrt{\tau} & \tau \leq 1 \\ -\frac{1}{4}[\log \frac{1+\sqrt{1-\tau^{-1}}}{1-\sqrt{1-\tau^{-1}}} - i\pi]^2 & \tau > 1 \end{cases}. \quad (2.4)$$

The K-factor for the gluon-gluon fusion process comes mainly from high order QCD corrections, which is not affected by the modified Yukawa coupling factor.

Other main production processes include the vector-boson-fusion (VBF) process, the associated production with  $W/Z$  bosons ( $WH/ZH$  process), and the associated Higgs production with heavy top quarks ( $t\bar{t}H$  process). The VBF process and  $WH/ZH$  processes are unaffected by the modified Yukawa coupling as there is no Yukawa coupling in these processes. They are dominant production channels in the fermiophobic Higgs model in which the gluon-gluon fusion process disappears. For the  $t\bar{t}H$  process which depends on the Yukawa coupling, due to its small portion, the impact from modified Yukawa coupling can be neglected safely although we really consider it in our calculation.

For Higgs decays, the 125 GeV SM Higgs decays mainly to  $b\bar{b}$ . The decay width is highly suppressed when  $F_{Y_u}$  approaches to zero. The Born level decay width  $\Gamma(H \rightarrow f\bar{f})$  can be calculated by:

$$\Gamma(H \rightarrow f\bar{f}) = \frac{G_F N_c}{4\sqrt{2}\pi} F_{Y_u}^2 M_H m_f^2 \beta_f^3, \quad (2.5)$$

where  $N_c = 3$ ,  $m_f$  is the fermion mass, and  $\beta = (1 - 4m_f^2/M_H^2)^{1/2}$ .

Although the branching ratio is small, the  $H \rightarrow \gamma\gamma$  process is one of the most promising channels for a low mass Higgs search at LHC due to its clean and simple final state topology, as well as the precise photon reconstruction on CMS and ATLAS detectors. The  $H \rightarrow \gamma\gamma$  process is a combination of both  $W$  and top quark triangle loops, whose decay width can be described as:

$$\Gamma(H \rightarrow \gamma\gamma) = \frac{G_F \alpha^2 M_H^3}{128\sqrt{2}\pi^3} \left| \sum_f N_c Q_f^2 F_{Y_u} A_{1/2}^H(\tau_f) + A_1^H(\tau_W) \right|^2, \quad (2.6)$$

where  $Q_f$  is the quark's charge,  $A_{1/2}^H(\tau)$  and  $A_1^H(\tau)$  are form factors for the spin 1/2 and spin 1 particles respectively, and  $\tau_i = M_H^2/4M_i^2$  with  $i = f, W$ .  $A_{1/2}^H(\tau)$  is given in eq. (2.3).

$$A_1^H(\tau) = -[2\tau^2 + 3\tau + 3(2\tau - 1)f(\tau)]\tau^{-2}, \quad (2.7)$$

$f(\tau)$  is given in eq. (2.4). As  $A_1^H(\tau_W)$  has an opposite minus sign to  $A_{1/2}^H(\tau_f)$ , the conjugation term between fermions and  $W$  bosons is suppressed when  $0 < F_{Y_u} < 1$ . Thus, the  $\Gamma(H \rightarrow \gamma\gamma)$  will increase when  $F_{Y_u}$  approaches zero.

In this paper, we do not consider the case when  $F_{Y_u} < 0$ . In most cases, the cross sections are proportional to  $|F_{Y_u}|^2$ . The only difference for a negative  $F_{Y_u}$  is happened in the  $H \rightarrow \gamma\gamma$  decay, as shown in equation (2.6). For a positive  $F_{Y_u} < 1$ ,  $\Gamma(H \rightarrow \gamma\gamma)$  is increased by reducing the minus conjugation term between  $W$  and fermion loops; For a negative  $F_{Y_u}$ , the conjugation term between  $W$  and fermion loop is positive, so the  $\Gamma(H \rightarrow \gamma\gamma)$  is increased. Related discussion can be found in [19, 20].

The  $H \rightarrow WW^*/ZZ^*$  processes are not affected by modifying the Yukawa factor.

By suppressing Yukawa couplings, the dominant production process  $gg \rightarrow H$  can be reduced. Meanwhile, the SM dominant decay mode,  $\Gamma(H \rightarrow b\bar{b})$  becomes small so the total decay width decrease.  $\Gamma(H \rightarrow \gamma\gamma)$  can be increased by reducing the cancelation between  $W$  and top quark loops. The branching ratio  $\text{Br}(H \rightarrow \gamma\gamma)$  is increased. In all, by introducing the modified Yukawa factor  $0 < F_{Y_u} < 1$ , the decrease range of  $\sigma(gg \rightarrow H)$  can be nearly the same as the increase range of  $\text{Br}(H \rightarrow \gamma\gamma)$  to make their product almost stable, which has been shown explicitly in table 1 for  $F_{Y_u} = 0$ .

### 3 Numerical results

In this Section, we shows the comparisons between the theoretical results after introducing the Yukawa factor  $F_{Y_u}$  and the experimental constraints. The SM Higgs production cross sections and their corresponding errors are taken from the state-of-art estimations by CERN

Higgs Cross section Working Group [23]. The Higgs decay branching ratios are calculated by using the HDECAY package [24] with modifying the Yukawa factor according to formulae described in section 2. The SM parameters are taken as  $G_F = 1.16637 \times 10^{-5} \text{ GeV}^{-2}$ ,  $\alpha_s(m_Z) = 0.119$ , and  $m_t = 172.5 \text{ GeV}$ . The Higgs mass is fixed at 125 GeV by default.

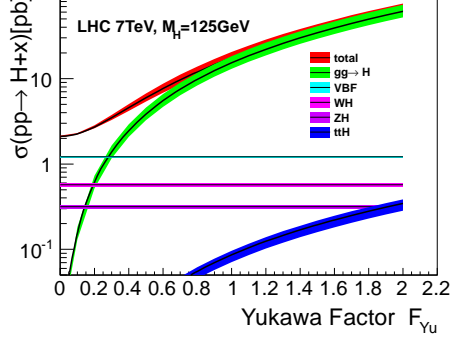


**Figure 1.** Higgs production cross section versus Yukawa factor  $F_{Y_u}$  at the LHC.

Figure 1 shows the production cross section of Higgs boson versus the modified Yukawa factor  $F_{Y_u}$ . It can be seen that the gluon-gluon fusion process is greatly impacted by this factor. The total cross section is mainly composed of gluon-gluon fusion when  $F_{Y_u} > 0.3$ . When  $F_{Y_u} < 0.2$ ,  $\sigma(pp \rightarrow H + x)$  is mainly contributed by VBF,  $WH$  and  $ZH$  processes, which are independent of the variation of  $F_{Y_u}$ . The  $\sigma(pp \rightarrow ZH + X)$  is about half of the  $\sigma(pp \rightarrow WH + X)$ , which is mainly caused by  $W/Z$  different couplings to quarks. The  $t\bar{t}H$  channel's contribution is less than 1% even though its value can be comparable with  $ZH$  process when  $F_{Y_u} \sim 2$ .

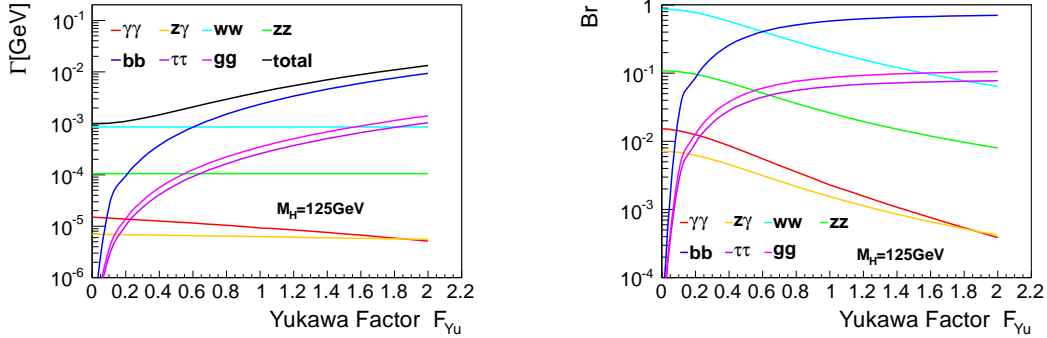


**Figure 2.** Higgs decay widths and branching ratios versus Yukawa factor  $F_{Y_u}$ .

Figure 2 shows the decay widths and the branching ratios for different Higgs decay modes versus  $F_{Y_u}$ . These channels can be divided into 3 categories.

1. The gauge boson decay mode  $H \rightarrow WW^*/ZZ^*$  whose partial decay widths are insensitive to  $F_{Y_u}$ .

2. The  $H \rightarrow \gamma\gamma$  and  $Z\gamma$  channels which are partly impacted by  $F_{Y_u}$ . These channels are contributed by both  $W$  and heavy fermion loops. Only the fermion-Higgs vertex in the triangle diagrams are affected.
3. The  $H \rightarrow b\bar{b}$ ,  $\tau\tau$  and  $gg$  channels which are sensitively affected. Their decay widths are proportional to  $F_{Y_u}^2$ .

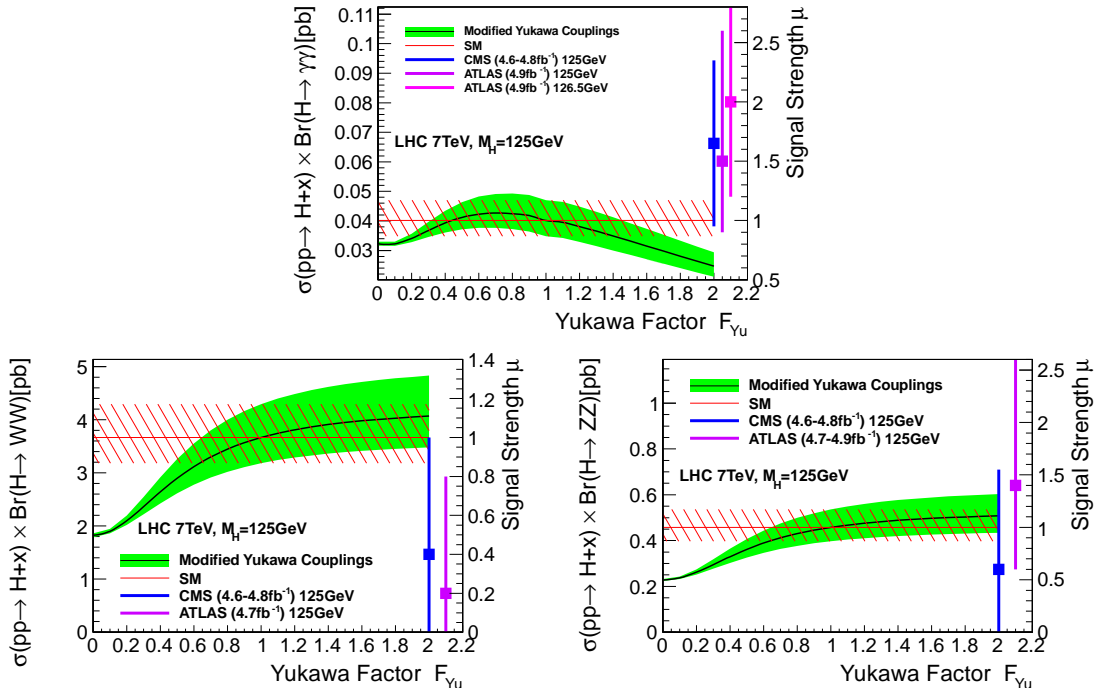


**Figure 3.** Higgs observable cross sections ( $\sigma \times \text{Br}$ ) versus Yukawa factor  $F_{Y_u}$  for  $H \rightarrow \gamma\gamma$ ,  $WW^*$ ,  $ZZ^*$  channels (black curve). The green hatched region presents the uncertainties. The SM value ( $F_{Y_u} = 1$ ) and its uncertainties are highlighted with the red line plus red hatched region for a convenient comparison. The square points with error bars show the CMS and ATLAS experimental results of the best-fit signal strength value  $\mu = \sigma/\sigma_{SM}$  as labeled on the right side Y-axis. Same conventions applied in the following plots.

Comparisons of the model predictions and the experimental results are given in Figure 3, 4, 5 and 6. For the modified Yukawa couplings, we have only considered uncertainties from the production cross section which are linear combination of the QCD scale and PDF +  $\alpha_s$  uncertainties [23]. For the hadron collider experimental results, they are taken from the best-fit of signal strength  $\mu = \sigma/\sigma_{SM}$  figures, as shown in table 2. By assuming the same selection efficiency as the SM signal, they can be compared directly to the production cross sections in our scenario, with normalized by SM production cross sections. Although curves and SM predicted values in our figures are drawn mostly with  $M_H = 125\text{ GeV}$ , the experimental data of the excess peaks can have small shifts. For example, the ATLAS excess peak in  $H \rightarrow \gamma\gamma$  channel is located at 126.5 GeV, whose signal strength is sensitive to this mass shift. To be clear, we show both  $M_H = 125\text{ GeV}$

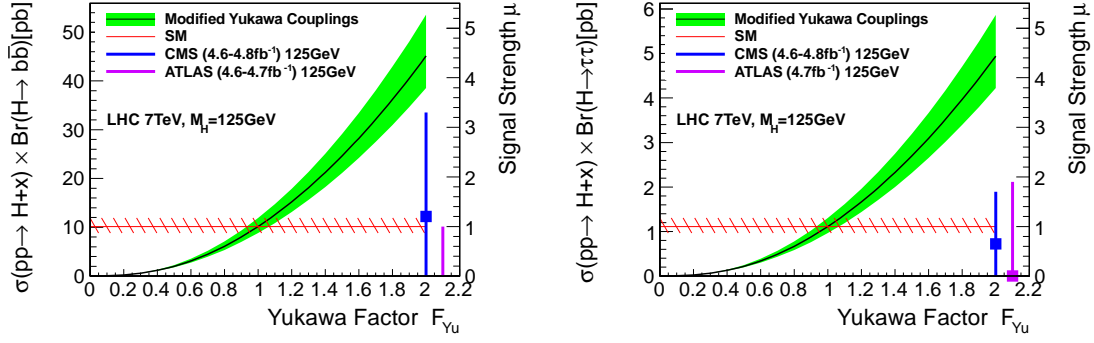


**Figure 4.** Higgs observable cross sections ( $\sigma \times \text{Br}$ ) versus Yukawa factor  $F_{Y_u}$  for  $H \rightarrow b\bar{b}/\tau\tau$  channels.

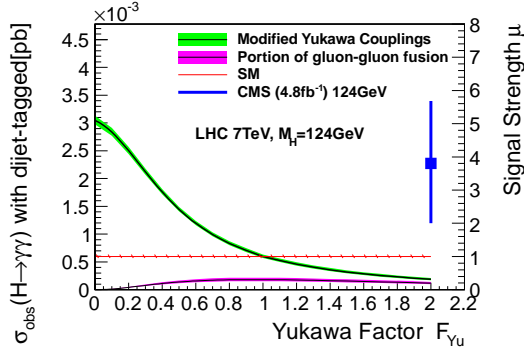


**Figure 5.**  $H \rightarrow \gamma\gamma$  observable cross sections with dijet-tagged versus Yukawa factor  $F_{Y_u}$ . The cross sections are obtained by  $\sigma_{VBF}(pp \rightarrow H + x)\text{Br}(H \rightarrow \gamma\gamma) \cdot 15\% + \sigma_{gg-fusion}(pp \rightarrow H + x)\text{Br}(H \rightarrow \gamma\gamma) \cdot 0.5\%$ , in which 15%(0.5%) is the efficiency for VBF(gg-fusion) process[25]. The black curve with purple hatched region shows the gg-fusion portion.

and 126.5 GeV  $\mu$  values in table 2 and figure 3. In principle, curve should be drawn with  $M_H = 126.5$  GeV to compare with the same Higgs mass experimental  $\mu$  data. However, for the inclusive Higgs production with diphoton decay, the SM observation cross sections are  $\sigma \cdot \text{Br}(H \rightarrow \gamma\gamma) = 17.50 \times 2.29 \times 10^{-3} = 0.0401$  pb for  $M_H = 125$  GeV and  $\sigma \cdot \text{Br}(H \rightarrow \gamma\gamma) = 17.07 \times 2.29 \times 10^{-3} = 0.0391$  pb for  $M_H = 126.5$  GeV [23]. So the difference between the small mass split can be safely neglected. Another special case is the CMS  $H \rightarrow \gamma\gamma$  with dijet-tagged, which corresponds to  $M_H = 124$  GeV. Similar as the above explanation, it is a good approximation to neglect the small difference between  $M_H = 124$  or 125 GeV in the comparison. Expect the two cases discussed above, the signal strength  $\mu$  are insensitive to the small mass shift and they are taken with  $M_H = 125$  GeV.

For  $H \rightarrow \gamma\gamma$  channel with  $F_{Y_u}$  increases from 0 to 2, the production cross section increases and  $\text{Br}(H \rightarrow \gamma\gamma)$  decreases, which makes  $\sigma(pp \rightarrow H + X) \cdot \text{Br}(H \rightarrow \gamma\gamma)$  change slowly around the SM predicted value 0.04pb. Thus, the SM and our modified Yukawa scenario will be indistinguishable in the inclusive  $H \rightarrow \gamma\gamma$  decay mode.



	CMS	ATLAS	Tevatron
$H \rightarrow \gamma\gamma$	$1.65^{+0.7}_{-0.7}[1]$	$2.0^{+0.8}_{-0.8} _{M_H=126.5\text{GeV}}[2]$ $1.5^{+0.9}_{-0.6}[2]$	...
$H \rightarrow W^+W^-$	$0.4^{+0.6}_{-0.6}[1]$	$0.2^{+0.6}_{-0.7}[2]$	...
$H \rightarrow ZZ$	$0.6^{+0.95}_{-0.6}[1]$	$1.4^{+1.2}_{-0.8}[2]$	...
$H \rightarrow b\bar{b}$	$1.2^{+2.1}_{-1.9}[1]$	$-0.8^{+1.8}_{-1.7}[2]$	...
$H \rightarrow \tau\tau$	$0.65^{+1.05}_{-1.3}[1]$	$0.0^{+1.9}_{-1.9}[2]$	...
$H \rightarrow \gamma\gamma$ with dijet-tagged	$3.8^{+2.4}_{-1.8} _{M_H=124\text{GeV}}[25]$	...	...
$WH/ZH, H \rightarrow b\bar{b}$	...	...	$2.0^{+0.8}_{-0.6}[5]$

**Table 2.** A collection of best-fit of signal strength  $\mu = \sigma/\sigma_{SM}$  experimental data. The values are read at  $M_H = 125$  GeV by default and special cases are labeled otherwise.

For  $H \rightarrow WW^*$  or  $ZZ^*$ , they both have very similar curves on the plots. The 125 GeV Higgs decays at least into one off-shell gauge boson due to it is under the threshold mass. The only difference is,  $\text{Br}(H \rightarrow WW^*)$  is about 10 times of  $\text{Br}(H \rightarrow ZZ^*)$ . So their observable cross sections can have about one order difference. The current  $WW^*/ZZ^*$  experimental results do not have enough precision to fix  $F_{Y_u}$  although  $H \rightarrow WW^*$  tends to be smaller than the SM prediction.

The information of the direct Yukawa coupling measurement channels  $H \rightarrow b\bar{b}$  and  $H \rightarrow \tau\tau$  at the LHC [3, 4] are shown in figure 4. Large Yukawa factor  $F_{Y_u}$  region ( $F_{Y_u} > 2$ ) can be excluded by current experimental results, but the error bar is too large to give a strict constraint on the  $F_{Y_u}$ .

As we have emphasized above, the pure gauge boson  $\gamma\gamma$ ,  $WW^*$  and  $ZZ^*$  Higgs decay channels may have difficulties to distinguish fermiophobic or our modified Yukawa models from the SM. Another complimentary mode is the VBF Higgs production and its decay into two photons, which makes the main contribution in Figure 5 (Part of Higgs produced by gg-fusion can also pass the dijet-tagging selection cuts as shown in the figure). The advantage of the VBF production channel is, its production cross section does not change with  $F_{Y_u}$ . The component of  $\sigma_{VBF}(pp \rightarrow H + x) \cdot \text{Br}(H \rightarrow \gamma\gamma)$  just exhibits the variation of the branching ratio  $\Gamma(H \rightarrow \gamma\gamma)$  with  $F_{Y_u}$ . By tagging the two forward jets, CMS has given the corresponding results [25] for 124 GeV Higgs and there can be about  $1.5\sigma$  deviation from the SM predicted values. It agrees well with our scenario when  $F_{Y_u} \sim 0.3$ . If this deviation can be confirmed in future experiments, it will be the direct evidence to support a smaller Yukawa factor rather than the SM.

Recently, Tevatron has also released their results on Higgs search [5]. Broad excess has been observed in the  $WH/ZH, H \rightarrow b\bar{b}$  channel. Tevatron data in the table 2 is a combination result for  $H \rightarrow b\bar{b}$ , which is dominantly contributed by  $ZH \rightarrow llb\bar{b}$  process [5]. This channel is important to fix  $F_{Y_u}$  for our scenario as it has direct  $Hb\bar{b}$  Yukawa coupling. The signal strength  $\sigma/\sigma_{SM}$  for 125 GeV Higgs as been shown in figure 6. There is no overlap between our selected  $F_{Y_u}$  region and the experimental data.

The estimated  $F_{Y_u}$  parameter regions within one standard deviation for all decay channels are summarized in table 3, which are extracted from the above figures. For a conserva-

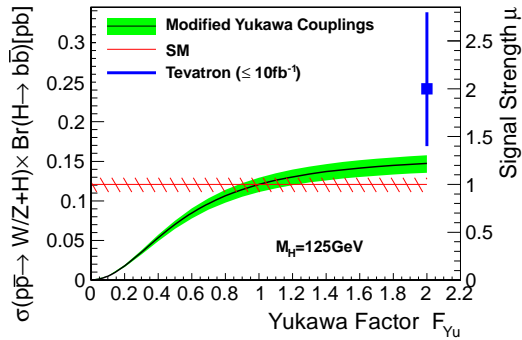


**Figure 6.** The  $WH/ZH, H \rightarrow b\bar{b}$  process at Tevatron with  $M_H = 125$  GeV.

Collider	Channels	$F_{Y_u}$ region
LHC	$H \rightarrow \gamma\gamma$	0.25-1.3
	$H \rightarrow W^+W^-$	0.0-1.0
	$H \rightarrow ZZ$	0.0-2.0
	$H \rightarrow b\bar{b}$	0.0-1.75
	$H \rightarrow \tau\tau$	0.0-1.35
	$H \rightarrow \gamma\gamma$ with dijet-tagged	0.0-0.6
Tevatron	$WH/ZH, H \rightarrow b\bar{b}$	...

**Table 3.** The allowed  $F_{Y_u}$  region by different experiment results.

tive estimation, value of  $F_{Y_u}$  can be taken within allowed region by CMS or ATLAS results. The comparison of the model predictions with the experimental data by each channel can exhibit the parameter dependence by different detection modes. For the complimentary research, we also show the  $\chi^2$  distribution variate with  $F_{Y_u}$  in Figure 7. The  $\chi^2$  is constructed as:

$$\chi^2 = \sum_i \left( \frac{\mu_i^{\text{the}} - \mu_i^{\text{exp}}}{\delta_i} \right)^2, \quad (3.1)$$

in which  $\mu_i^{\text{the}}$  are theoretical predicted signal strength as the observation cross sections normalized by the SM cross sections,  $\mu_i^{\text{exp}}$  are experimental data as shown in the table 2.  $\delta_i$  are experimental errors and are taken as the average values for asymmetric errors. The optimal  $F_{Y_u}$  value, which corresponds the  $\chi^2_{\min}$ , is 0.3(0.6) for Tevatron included(excluded) data sample. Roughly speaking, a suppression effects with about half of the SM Yukawa coupling strength can obtain a optimal global fit.

## 4 Conclusion

LHC has already observed some possible excesses in the Higgs search at about 125 GeV. For a deeper understanding of the gauge symmetry breaking and the origins of mass, it is necessary to study phenomenologically the properties of this possible 125 GeV Higgs. In this

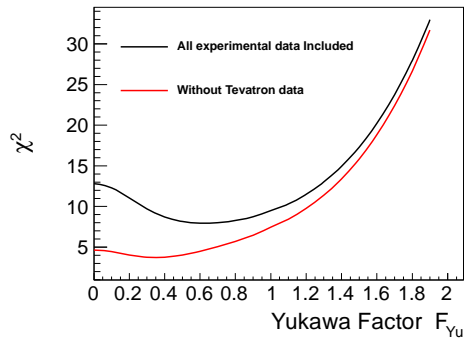


**Figure 7.** The  $\chi^2$  fit to find the optimal Yukawa factor  $F_{Y_u}$ . For the black curve, all experimental data in table 2 except ATLAS inclusive  $H \rightarrow \gamma\gamma$  with  $M_H = 126.5$  GeV are used. For the red curve, Tevatron experimental data is also excluded.

paper, we focus on the Yukawa coupling between Higgs and fermions. By introducing an effective universal Yukawa coupling scale factor, we show that at the LHC, the production cross section  $\sigma(pp \rightarrow H + x)$  and the branching ratio  $\text{Br}(H \rightarrow \gamma\gamma)$  can change oppositely to make their product almost stable. The inclusive  $H \rightarrow \gamma\gamma$  information is not capable of distinguishing between the modified Yukawa scenario and the SM. Due to tagging and reconstructing difficulties, the current LHC  $H \rightarrow b\bar{b}$  or  $\tau\tau$  data are not precise enough to examine the Yukawa coupling directly. CMS has observed possible deviation from the SM prediction in the vector-boson-fusion Higgs production with diphoton decay. This can be explained by a suppressed effective Yukawa coupling. Our investigation shows that, the global  $\chi^2$  fit can get its optimal value by introducing a suppression factor  $F_{Y_u} \sim 1/2$  on the SM Yukawa couplings. Limited by the information of the experimental data,  $F_{Y_u} \sim 1/2$  is a very rough estimation. Future higgs search measurements can crosscheck this estimation and possible model construction work can be made to suppress the Yukawa couplings.

**Note Added:** While our paper has been completed, we noticed the paper [20], which also studied the Higgs properties from the LHC and Tevatron data.

## 5 Supplement

Before the publication of this paper, ATLAS and CMS at the LHC announced the discovery of a new higgs-like boson at a mass near 125 GeV[26–29]. Therefore, it is necessary to include the latest experimental results in this research. To keep the self-completeness of the previous analysis, we make the update analysis in this supplement section.

Figure 8 shows the comparison of the Higgs production cross sections versus  $F_{Y_u}$  with  $\sqrt{s} = 7$  TeV and 8 TeV. The SM Higgs production cross sections at 8 TeV and their corresponding errors are taken from the state-of-art estimations by CERN Higgs Cross Section Working Group [30]. For  $m_H = 125$  GeV, the SM Higgs production cross section at 8 TeV is about 1.27 times of that at 7 TeV. The Higgs decay width and branching ratio are independent of the LHC energy as already shown in figure 2.

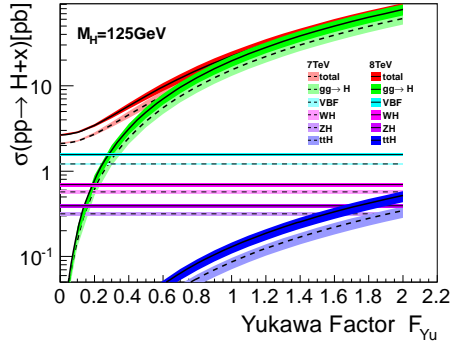


**Figure 8.** Higgs production cross section versus Yukawa factor  $F_{Y_u}$  at the LHC for both  $\sqrt{s}=7\&8$  TeV. The solid (dashed) lines with (light) shaded regions show the cross sections at 8 TeV (7 TeV).

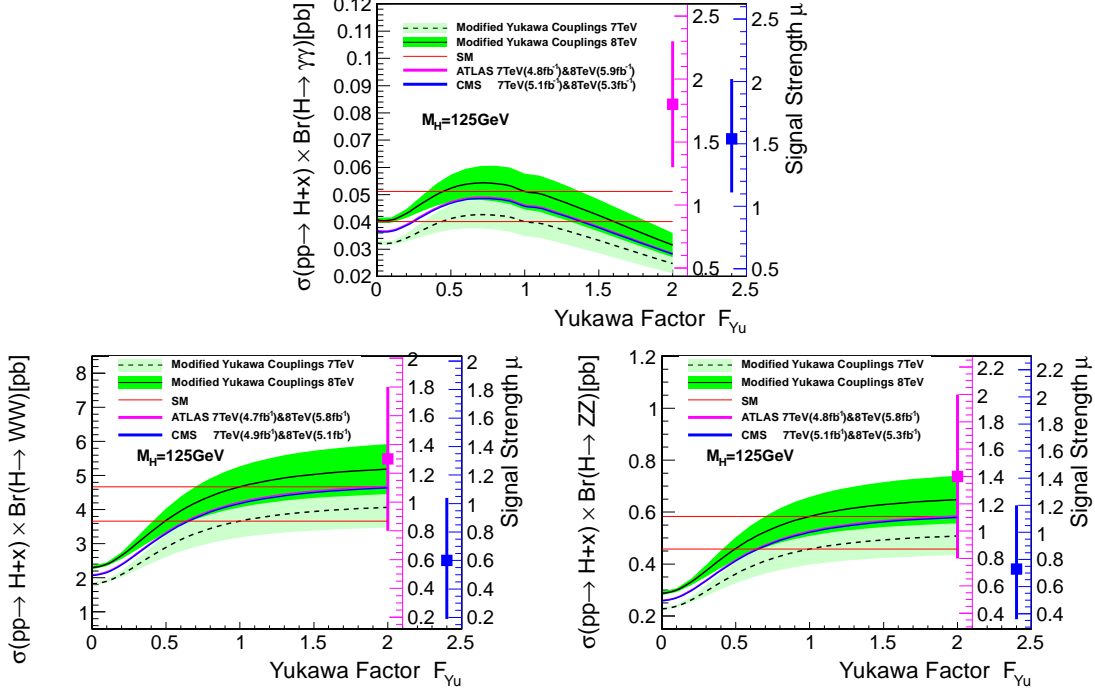
To compare the model predictions with the experimental results, we collect the best-fit values of signal strength  $\mu$  from the experimental data in table 4. To be consistent, all signal strengths  $\mu$  of different channels for ATLAS and CMS are taken as the 7&8 TeV combined results, also shown are their integrated luminosities at 7&8 TeV. The corresponding Higgs mass may have a small (+0.5 GeV or +1.0 GeV) but ignorable difference from 125 GeV.

	CMS		ATLAS	
	$\mu$	$\mathcal{L}(7\&8\text{TeV})$	$\mu$	$\mathcal{L}(7\&8\text{TeV})$
$H \rightarrow \gamma\gamma$	$1.54^{+0.48}_{-0.43}$ [29]	$5.1\text{fb}^{-1}\&5.3\text{fb}^{-1}$ [29]	$1.8 \pm 0.5$ [27]	$4.8\text{fb}^{-1}\&5.9\text{fb}^{-1}$ [27]
$H \rightarrow W^+W^-$	$0.60^{+0.44}_{-0.41}$ [29]	$4.9\text{fb}^{-1}\&5.1\text{fb}^{-1}$ [29]	$1.3 \pm 0.5$ [27]	$4.7\text{fb}^{-1}\&5.8\text{fb}^{-1}$ [27]
$H \rightarrow ZZ$	$0.73^{+0.47}_{-0.37}$ [29]	$5.1\text{fb}^{-1}\&5.3\text{fb}^{-1}$ [29]	$1.4 \pm 0.6$ [27]	$4.8\text{fb}^{-1}\&5.8\text{fb}^{-1}$ [27]
$H \rightarrow b\bar{b}$	$0.47^{+0.85}_{-0.71}$ [29]	$5.0\text{fb}^{-1}\&5.1\text{fb}^{-1}$ [29]	...	...
$H \rightarrow \tau\tau$	$0.08^{+0.79}_{-0.76}$ [29]	$4.9\text{fb}^{-1}\&5.1\text{fb}^{-1}$ [29]	...	...
VBF, $H \rightarrow \gamma\gamma$	$2.13^{+1.32}_{-1.09}$ [28]	$5.1\text{fb}^{-1}\&5.3\text{fb}^{-1}$ [28]	...	...
VH, $H \rightarrow b\bar{b}$	$0.52^{+0.84}_{-0.80}$ [28]	$5.0\text{fb}^{-1}\&5.1\text{fb}^{-1}$ [28]	...	...

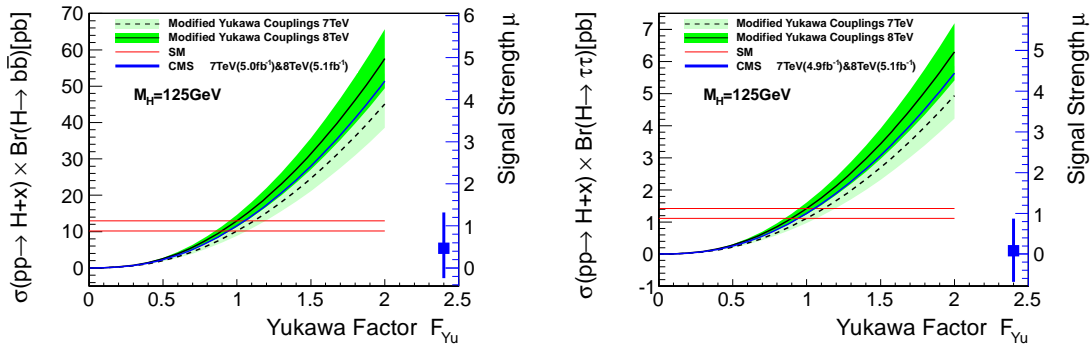
**Table 4.** A collection of 7&8 TeV combined best-fit values of signal strength  $\mu = \sigma/\sigma_{SM}$  from experimental data, together with the integrated luminosities at 7&8 TeV.

Figure 9, 10 and 11 show the comparison of the model predictions and the experimental results for different Higgs production and decay modes. The model predicted observable cross section at 8/7 TeV is drawn as the black/dashed curve with green/light green error band. The SM predicted central values are shown as the horizontal red line for both 7 and 8 TeV cases. The 7 and 8 TeV curves should be combined together to compare with the experimental signal strength listed in table 4. This is shown as the magenta/blue curve for the ATLAS/CMS. For simplicity, this combination is done by adding 7 TeV and 8 TeV predicted values with different weights proportional to their corresponding luminosities. As ATLAS and CMS may have different luminosities for 7 and 8 TeV in the combination, their combined results maybe different and should be compared with their individual

experimental results, with different axis-labels, as shown on the right side of each plot.



**Figure 9.** Higgs observable cross sections ( $\sigma \times \text{Br}$ ) versus Yukawa factor  $F_{Y_u}$  for  $H \rightarrow \gamma\gamma, WW^*, ZZ^*$  channels (black/dashed curve for 8/7 TeV). The green shaded region presents the uncertainties. The SM value ( $F_{Y_u} = 1$ ) are shown with the red lines for both 7&8 TeV cases. The 7&8 TeV combined predictions are drawn in magenta/blue for ATLAS/CMS. The magenta/blue square points with error bars show the ATLAS/CMS experimental results of the best-fit signal strength value  $\mu = \sigma/\sigma_{SM}$ , which are labeled on the right side Y-axis individually. Same conventions applied in the following plots.



**Figure 10.** Higgs observable cross sections ( $\sigma \times \text{Br}$ ) versus Yukawa factor  $F_{Y_u}$  for  $H \rightarrow b\bar{b}/\tau\tau$  channels.

In table 5, we show the allowed  $F_{Y_u}$  region by different channels for 7&8 TeV results,

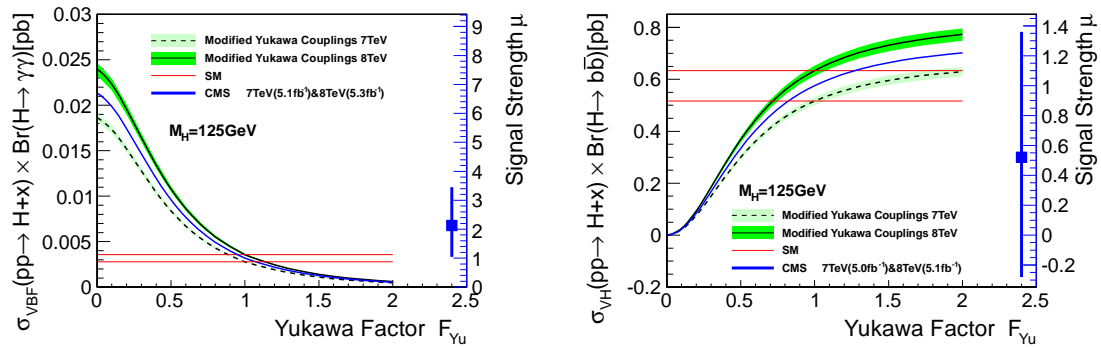


**Figure 11.** Higgs observable cross sections versus Yukawa factor  $F_{Y_u}$  for VBF  $H \rightarrow \gamma\gamma$  /  $VH \rightarrow b\bar{b}$ .

obtained from the above figures. It suggests that an universal suppressed Yukawa coupling factor can increase signal strength easily in VBF,  $H \rightarrow \gamma\gamma$  channel. However, it maybe difficult to increase the signal strength in the inclusive  $H \rightarrow \gamma\gamma$  channel. A global  $\chi^2$  fit can also be made as shown in equation (3.1). The input data are taken from table 4. Results are shown in the figure 12, with optimal  $F_{Y_u} \sim 0.65$ . This is consistent with the global fit result by CMS collaboration [28].

Channels	$F_{Y_u}$ region
$H \rightarrow \gamma\gamma$	0
$H \rightarrow W^+W^-$	0.0-2.0
$H \rightarrow ZZ$	0.0-2.0
$H \rightarrow b\bar{b}$	0.0-1.1
$H \rightarrow \tau\tau$	0.0-0.9
VBF, $H \rightarrow \gamma\gamma$	0.4-1.0
$VH, H \rightarrow b\bar{b}$	0.0-2.0

**Table 5.** The allowed  $F_{Y_u}$  region by different experiment results.

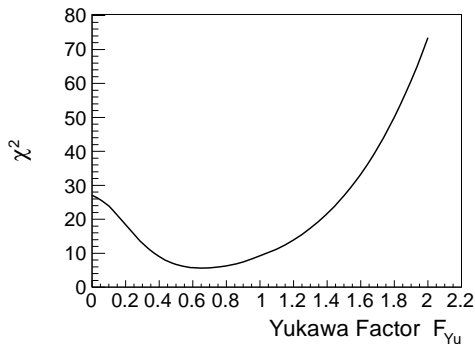


**Figure 12.** The  $\chi^2$  fit to find the optimal Yukawa factor  $F_{Y_u}$ .

## Acknowledgements

This research is supported in part by the Natural Science Foundation of China under grant numbers 11075003, 10821504, 11075194, and 11135003, by the Postdoctoral Science Foundation of China under grant number Y2Y2231B11, and by the DOE grant DE-FG03-95-Er-40917.

## References

- [1] CMS collaboration, *Combination of SM, SM 4, FP Higgs boson searches*, CMS-PAS-HIG-12-008, CERN, Geneva Switzerland (2012).
- [2] ATLAS collaboration, *An update to the combined search for the Standard Model Higgs boson with the ATLAS detector at the LHC using up to  $4.9 \text{ fb}^{-1}$  of  $pp$  collision data at  $\sqrt{s} = 7 \text{ TeV}$* , ATLAS-CONF-2012-019, CERN, Geneva Switzerland (2012).
- [3] CMS collaboration, A. Bornheim, *Searches for the Standard Model Higgs Boson at CMS, presentation at the XLVII<sup>th</sup> Rencontres de Moriond session devoted to QCD and high energy interactions, Higgs session*, La Thuile Italy March 10 2012.
- [4] ATLAS collaboration, R. Bernhard, *Searches for the Standard Model Higgs Boson at ATLAS, presentation at the XLVII<sup>th</sup> Rencontres de Moriond session devoted to QCD and high energy interactions, Higgs session*, La Thuile Italy March 10 2012.
- [5] TEVNP Working Group collaboration, *Combined CDF and D0 search for Standard Model Higgs boson production with up to  $10.0 \text{ fb}^{-1}$  of data*, FERMILAB-CONF-12-065-E, Fermilab Batavia U.S.A. (2012) [CDF-Note-10806] [D0-Note-6303] [arXiv:1203.3774].
- [6] J. Basdevant, E. L. Berger, D. Dicus, C. Kao, and S. Willenbrock, *Final state interaction of longitudinal vector bosons*, *Phys. Lett.* **B313** (1993) 402 [arXiv:hep-ph/9211225].
- [7] V. D. Barger, N. Deshpande, J. Hewett, and T. Rizzo, *A separate Higgs?*, arXiv:hep-ph/9211234.
- [8] P. Bamert and Z. Kunszt, *Gauge boson masses dominantly generated by Higgs triplet contributions?*, *Phys. Lett.* **B306** (1993) 335 [arXiv:hep-ph/9303239].
- [9] H. Pois, T. J. Weiler, and T. C. Yuan, *Higgs boson decay to four fermions including a single top quark below  $t\bar{t}$  threshold*, *Phys. Rev.* **D47** (1993) 3886 [arXiv:hep-ph/9303277].
- [10] A. Stange, W. J. Marciano, and S. Willenbrock, *Higgs bosons at the Fermilab Tevatron*, *Phys. Rev.* **D49** (1994) 1354 [arXiv:hep-ph/9309294].
- [11] M. A. Diaz and T. J. Weiler, *Decays of a fermiophobic Higgs*, arXiv:hep-ph/9401259.
- [12] A. Akeroyd, *Fermiophobic Higgs bosons at the Tevatron*, *Phys. Lett.* **B368** (1996) 89 [arXiv:hep-ph/9511347].
- [13] A. Akeroyd, *Fermiophobic and other nonminimal neutral Higgs bosons at the LHC*, *J.Phys.G* **G24** (1998) 1983 [arXiv:hep-ph/9803324].
- [14] E. Gabrielli and B. Mele, *Testing effective Yukawa couplings in Higgs searches at the Tevatron and LHC*, *Phys. Rev.* **D82** (2010) 113014 [Erratum *ibid.* **D** 83 (2011) 079901] [arXiv:1005.2498].
- [15] E. Gabrielli and B. Mele, *A radiatively improved fermiophobic Higgs boson scenario*, arXiv:1112.5993.



- [16] E. Gabrielli, B. Mele, and M. Raidal, *Has a fermiophobic Higgs boson been detected at the LHC?*, *Phys. Lett. B* **716** (2012) 322 [arXiv:1202.1796].
- [17] CMS collaboration, *Search for the fermiophobic model Higgs boson decaying into two photons*, CMS PAS HIG-12-002, CERN, Geneva Switzerland (2012).
- [18] ATLAS collaboration, *Search for a fermiophobic Higgs boson in the diphoton decay channel with  $4.9 \text{ fb}^{-1}$  of ATLAS data at  $\sqrt{s} = 7 \text{ TeV}$* , ATLAS-CONF-2012-13, CERN, Geneva Switzerland (2012).
- [19] J. Espinosa, C. Grojean, M. Muhlleitner, and M. Trott, *Fingerprinting Higgs suspects at the LHC*, *JHEP* **05** (2012) 097 [arXiv:1202.3697].
- [20] P. P. Giardino, K. Kannike, M. Raidal, and A. Strumia, *Reconstructing Higgs boson properties from the LHC and Tevatron data*, *JHEP* **06** (2012) 117 [arXiv:1203.4254].
- [21] C. Quigg, *Unanswered questions in the electroweak theory*, *Ann. Rev. Nucl. Part. Sci.* **59** (2009) 505 [arXiv:0905.3187].
- [22] A. Djouadi, *The anatomy of electro-weak symmetry breaking. I: The Higgs boson in the Standard Model*, *Phys. Rept.* **457** (2008) 1 [arXiv:hep-ph/0503172].
- [23] LHC Higgs Cross section Working Group collaboration, S. Dittmaier et al., *Handbook of LHC Higgs cross sections: 1. Inclusive observables*, arXiv:1101.0593, CERN-2011-002.
- [24] A. Djouadi, J. Kalinowski, and M. Spira, *HDECAY: a program for Higgs boson decays in the Standard Model and its supersymmetric extension*, *Comput. Phys. Commun.* **108** (1998) 56 [arXiv:hep-ph/9704448].
- [25] CMS collaboration, *Search for the Standard Model Higgs boson decaying into two photons in  $pp$  collisions at  $\sqrt{s} = 7 \text{ TeV}$* , CMS-HIG-11-033, CERN, Geneva Switzerland (2012) [CERN-PH-EP-2012-024] [*Phys. Lett. B* **710** (2012) 403] [arXiv:1202.1487].
- [26] ATLAS collaboration, *Observation of an excess of events in the search for the Standard Model Higgs boson with the ATLAS detector at the LHC*, ATLAS-CONF-2012-093, CERN, Geneva Switzerland (2012).
- [27] ATLAS collaboration, *Observation of a new particle in the search for the Standard Model Higgs boson with the ATLAS detector at the LHC*, CERN-PH-EP-2012-218, CERN, Geneva Switzerland (2012) [*Phys. Lett. B* **716** (2012) 1] [arXiv:1207.7214].
- [28] CMS collaboration, *Observation of a new boson with a mass near  $125 \text{ GeV}$* , CMS-PAS-HIG-12-020, CERN, Geneva Switzerland (2012).
- [29] CMS collaboration, *Observation of a new boson at a mass of  $125 \text{ GeV}$  with the CMS experiment at the LHC*, CMS-HIG-12-028, CERN, Geneva Switzerland (2012) [CERN-PH-EP-2012-220] [*Phys. Lett. B* **716** (2012) 30] [arXiv:1207.7235].
- [30] *Higgs production cross sections with errors*, presented in <https://twiki.cern.ch/twiki/bin/view/LHCPhysics/CERNYellowReportPageAt8TeV>, CERN, Geneva Switzerland (2012).